

Load Forecasting Based on Wavelet Submodel and LS-SVM

Song Qiang¹, Qin Tao^{2,3}

¹School of Mechanical Engineering, Anyang Institute of Technology, Anyang, 455000, China

²State Grid Shang Luo Power Supply Company, Shaanxi, Shangluo 726200, China

³State Grid Tongchuan Power Supply Company, Shaanxi, Tongchuan 727031, China
songqiang01@yeah.net

Received January 2018; revised October 2019

ABSTRACT. *The work studied chaotic characteristics and reasons of random quantity, quasi-periodic quantity and development trend quantity in the load after wavelet decomposition. Embedding dimension m and delay time of phase space reconstruction was determined based on the forecast accuracy of least squares support vector machines (LS-SVM). Meanwhile, each subsequence used LS-SVM for the forecasting of local chaos, thus obtaining final prediction value. The measured data analysis showed that the method, with high precision and good robustness of parameters, can obtain satisfactory results.*

Keywords: Short-term load forecasting; Least squares support vector machines (LS-SVM); Load submodel; Chaos; Predictable time

1. **Introduction.** It is believed that the load of power system consists of random quantity, quasi-periodic quantity (such as daily and weekly periodicities), seasonal variation quantity, and development trend quantity [1]. Meanwhile, the study shows the load has chaotic characteristics, and some prediction methods based on chaos use the load as a whole for forecasting [2-8]. However, unified modeling cannot well reflect the nonlinear law of time series of load, restricting forecasting accuracy. Double periods and chaos method are used in [9], without specific analysis of the interaction between sequences of different time scales. The extraction of Fourier transform with double periods is suitable for stable quantity, which affects the accuracy of calculation results.

The work analyzed interference of periodic quantity to chaos quantity, dividing them into three prediction submodels: random quantity, quasi-periodic quantity and development trend quantity. Wavelet transform was used to extract trend quantity, periodic quantity and random quantity in original signal. It could play a smoothing effect on the original signal, conducive to modeling and forecasting. Scale time series was extracted using the stationary wavelet transform, comprising three subsequences according to periods [10]. Set random time series to 0, local forecasting models of LS-SVM were constructed based on characteristics of the other two subsequences, respectively [11], [12]. The actual data calculation shows the rationality and correctness of analysis and method in the work.

2. Theoretical Basis.

2.1. **Stationary wavelet decomposition.** Stationary wavelet transform [10] performs the interpolation between the values of filters at all levels rather than double extraction of output coefficients of low-pass and high-pass filters. Thus, wavelet and scale coefficients have equal length to original signal, and the signal correspond to the original signal in

each resolution. It is important for the forecasting of time series. Set filter coefficients of high-pass and low-pass filters of orthonormal wavelet as

$$H_i = [h_{i,1}, \dots, h_{i,j}, \dots, h_{i,J}] \quad G_i = [g_{i,1}, \dots, g_{i,j}, \dots, g_{i,J}]$$

where subscripts i and j represent the j -th coefficient of the filter at the i -th level. Set $H_i = Z_i H_{i-1}$, $G_i = Z_i G_{i-1}$, and Z_i is the zerofill operator of interpolation, then $h_{i,2^i j} = h_{i-1,j}$; $h_{i,j} = 0$; $g_{i,2^i j} = g_{i-1,j}$; $g_{i,j} = 0$ (j is not equal to the integral multiple of 2^i). If s is the original signal sequence, and $a_0 = s$, then the deposition of the stationary wavelet transform is

$$a_{i+1} = H_i a_i, \quad b_{i+1} = G_i a_i \quad (i = 0, \dots, M)$$

where a_i is the scale coefficient; b_i the wavelet coefficient; M the maximum series of decomposition.

Using stationary wavelet to decompose load data, different submodels can be constituted. It can not only reduce the mutual interference, but also dip the internal laws of submodels.

2.2. LS_SVM regression model.

2.2.1. *SVMs*. Support vector machines (SVMs) proposed by Vapnik et al. [13] is one of the most influential outcomes in the field of machine learning. However, it needs to solve convex quadratic programming for SVM training. The obtained solution is the unique optimal one, but the complexity of the algorithm depends on the number of sample data. The bigger the sample data is, the slower the computation speed. Using LS_SVM is an effective solution [14]. LS_SVM improves convergence rate with better noise immunity by solving one system of linear equation instead of quadratic programming in SVM [15].

2.2.2. *LS_SVM regression model*. Let the training data set $\{x_t, y_t\}$, $t = 1, \dots, l$. $x_t \in \mathbb{R}^m$ is the input mode of the t -th sample; $y_t \in \mathbb{R}$ the desired output corresponding to the t -th sample; l the number of training samples. LS_SVM is defined as follows

$$y(x) = w^T \varphi(x) + b, \quad (1)$$

where non-linear transformation $\varphi(x)$ maps the input data into a high dimensional feature space. It is no need to pre-specify the dimension of w (which can be infinite). In LS_SVM, the objective function is defined as

$$\min J(w, e) = \frac{1}{2} w^T w + \gamma \frac{1}{2} \sum_{t=1}^N e_t^2 \quad (2)$$

The constraint is

$$y(x) = w^T \varphi(x_t) + b + e_t, \quad t = 1, \dots, N, \quad (3)$$

The first part in Eq. (2) is regularization, and the second part the empirical risk.

The objective function only has equality constraint, and the loss function in optimization targets is the second moment norm of error e_t , which will simplify the solution to the problem. Lagrangian function is defined as

$$L(w, b, e, \alpha) = J(w, e) - \sum_{t=1}^N \alpha_t \{w^T \varphi(x_t) + b + e_t - y_t\}, \quad (4)$$

where α_t is Lagrange multiplier. According to the optimal condition of Karush_Kuhn_Tucker (KKT), we eliminate e_t and w to $t=1, \dots, N$, deriving the following linear equation.

$$\begin{bmatrix} 0 & \mathbf{1}^T \\ \mathbf{1} & \varphi(x_t)^T \varphi(x_t) + \mathbf{D} \end{bmatrix} \begin{bmatrix} b \\ \alpha \end{bmatrix} = \begin{bmatrix} 0 \\ y \end{bmatrix}, \quad (5)$$

where $y = [y_1; \dots; y_N]^T$; $\mathbf{1} = [1; \dots; 1]^T$; $\alpha = [\alpha_1; \dots; \alpha_N]^T$; $\mathbf{D} = \text{diag}[\gamma_1; \dots; \gamma_N]$. Then the optimization problem of LS_SVM is transformed into linear Eq. (5) using LS for solution.

The selected kernel function satisfies Mercer condition.

$$\Psi(x_t, x_l) = \varphi(x_t)^T \varphi(x_l), t, l = 1, \dots, N, \quad (6)$$

Finally, the following LS_SVM regression model is obtained.

$$y(x) = \sum_{t=1}^N \alpha_t \psi(x, x_t) + b, \quad (7)$$

where α_t and b are the solutions of linear equation; $\Psi(x, x_t)$ represents the high-dimensional feature space from the nonlinear mapping of input space x . The work uses the commonly used radial basis function as the kernel function.

$$\psi(x_t, x_l) = \exp(-\|x - x_t\|_2^2 / \sigma^2) \quad (8)$$

where σ is the positive real constant.

There is similarity in the basic idea of SVM and reconstruction theory of state space. The vector of input space is extended to the high dimensional space, extracting information and laws hidden in the system. Therefore, SVM, used for the reconstruction of phase space, can automatically map the input vector into a high dimensional feature space. It can realize the separable data linearity to extract information, which has achieved good results in the forecasting of chaotic time series.

3. Construction of Three Subsequences of Load.

3.1. Load component analysis. Fig. 1 (1) is the annual load data of a city in northwest (with sampling period of 15min); Fig. 1 (2) the power spectrum of the load (horizontal axis is period).

Fig. 1 (2) shows the actual load periods are mainly 12h and 24h, including the periods with smaller amplitude such as 2h, 3h, 4h, 6h and 168h. It is decomposed into 7 layers with stationary db4 wavelet transform, reconstructing the loading value of each subsequence (See Fig. 2). The first layer is mainly random quantity, including chaos quantity as well. It can constitute stochastic model; the second to the sixth layers are the loads with the period from 2h to 24h, constructing quasi-periodic model; the seventh layer, although containing some loads with period of 24h, is unstable with considerable variation of amplitude. Therefore, it will constitute trend model with the remaining.

3.1.1. Chaotic characteristic analysis of the subsequences of the load. Stochastic model obtains its delay in accordance with mutual information method [16].

Time $\tau = 3$, and embedding dimension $m=11$ according to Cao method [17]. Lyapunov index is 0.0264 based on small data sets [18], revealing that it contains chaos quantity. There are lots of random quantities difficult to forecast, so it will be set to 0.

For periodic model, we can obtain $\tau = 15$; $m=8$; lyapunov index is 0.0717. The contained chaos quantity can be used for the forecasting of chaotic way.

For trend model, we can obtain $\tau = 21$; $m=5$; lyapunov index is 0.0553. The contained chaos quantity can be used for the forecasting of chaotic way.

It is generally believed chaos quantity is "seemingly random" however, even envelopment trend and quasi-periodic parts contain chaos quantity in the mentioned three submodels. The difference of load record and trend (a typical daily variation curve obtained by statistics, namely the basic load, is periodic quantity) is chaotic [19]. It is the reason that each scale show chaotic characteristics. The discrete rate of given track and adjacent trajectory, namely the growth rate of distance to adjacent trajectory, is calculated by Lyapunov

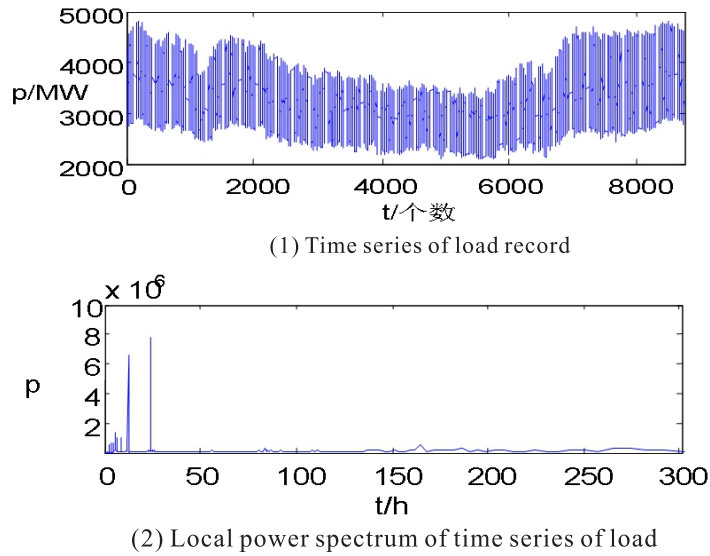


FIGURE 1. Time series of load and its time series of load

index. In the calculation of distance, the basic loads contained by the given trajectory points and adjacent points are mutually cancelled. Thus, it finally shows Lyapunov index around the fluctuation of basic load, existing in each scale. E.g., the load of d6 layer shows the period of 24h, and its Lyapunov index is 0.0242 after calculation.

The above analysis shows the reason that the load of power system contains chaos quantity is because daily load fluctuates around basic load. Chaos quantity is contained due to the fluctuation in scales.

3.2. Predictable time of load. Load can be divided into load trend (periodic quantity) and chaos quantity. Lyapunov index reflects the predictable time of chaos quantity instead of load trend. Therefore, the predictable time of the load, not only determined by Lyapunov index, should consider the influence of load trend.

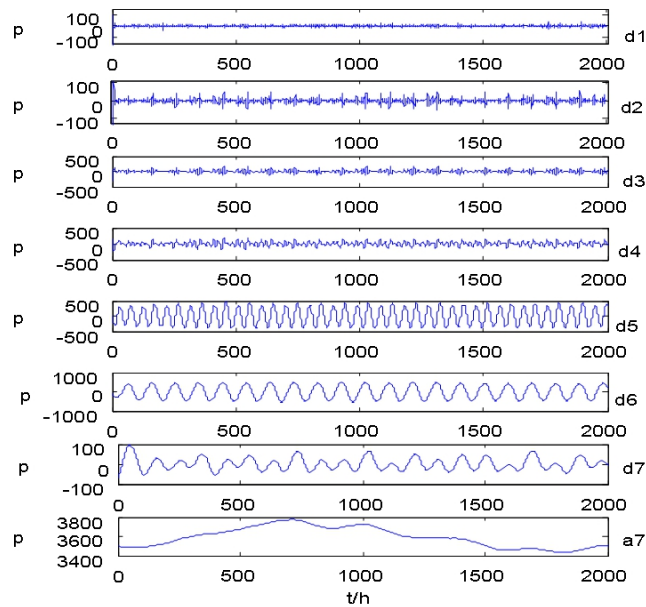


FIGURE 2. Wavelet decomposition of load

4. Prediction Algorithm of the Chaos Model of Three Subsequences.

4.1. **Selection of sampling period.** Shorter sampling period, reflecting more system information, increases the influence of noise. Furthermore, it will contain redundant information when the predictive step is large. The sampling period of load data is 15min in the work.

4.2. **Reconstruction of phase space.** Reconstruction of phase space should select embedding dimension m and delay time τ .

Embedding dimension m is not only the parameter of chaos quantity, but also the input dimension of LS-SVM. Increasing m can increase learning capacity for LS-SVM, thus improving learning effects and forecast accuracy. However, higher m will cause information redundancy as well as increasing error. The optimal embedding dimension to the actual data is derived by heuristics in the work.

Delay time τ of chaos quantity can be obtained by mutual information method. Based on time window, delay time should be decreased to increase the input dimension of LS-SVM.

Phase space is reconstructed.

$$\begin{bmatrix} x(1) & x(2) & \dots x(l) \\ x(1+\tau) & x(2+\tau) & \dots x(l+\tau) \\ \cdot & & \cdot \\ \cdot & & \cdot \\ x(1+(m-1)\tau) & x(2+(m-1)\tau) & \dots x(l+(m-1)\tau) \end{bmatrix}$$

where $[x(1), x(2), \dots, x(l+(m-1)\tau)]$ is the time series of load; l the number of phase space points.

$$X(k) = [x(k); x(k+\tau); \dots x(k+(m-1)\tau)]$$

Current load $x(k)$ should forecast the load after t steps, and then historical data is

$$\{X(k-t), X(k-t-1), \dots, X(k-t-(N-1))\}$$

After calculating the Euclidean distance between historical data and $X(k)$, n points with minimum distance are selected as input. The experiments show that $n=60$, and target data is $x(k+t)$, where t is predictive step.

Data sampling period is 15min in the work. $t = 1$ when we forecast the load after 15min; $t = 4$ when we forecast after 1h, and so on. N is the number of historical data, and the work used the data of the first 30 days.

4.3. **Parameter determination of LS-SVM.** The parameters (γ, σ) are determined by using adaptive parameter optimization method [20]. The algorithm is as follows:

- a. Value ranges of parameter γ and kernel parameter *sigma* are determined.
- b. Pair of Parameter $\{\gamma_i, \sigma_j : i = 1, \dots, m, j = 1, \dots, n\}$ is constructed, namely the value ranges of two parameters are regarded as m and n , constituting $m \times n$ pairs of parameters $\{\gamma_i, \sigma_j\}$;
- c. Each pair of parameters is substituted into LS-SVM to estimate accuracy. The parameter with the highest estimate accuracy is the optimal one $\{\gamma_i, \sigma_j\}$;
- d. If the error accuracy cannot meet the requirement, we take $\{\gamma_i, \sigma_j\}$ as the center to narrow the value range of parameters. Step c is repeated to constantly optimize the parameters of LS-SVM until the required error accuracy is satisfied.

Estimate accuracy is measured by root-mean-square error (R_{mse}):

$$R_{mse} = \sqrt{\frac{1}{n} \sum_{i=1}^n [x(i) - x'(i)]^2} \quad (9)$$

where x is the original signal; x' the estimate signal; n the number of data points[21,22]. In summary, the specific algorithm is as follows:

- (1) Historical data is recognized, amending abnormal data.
- (2) Stationary wavelet decomposition is performed to historical data, with the decomposition coefficient of each layer inversely transformed into load value.
- (3) Set the stochastic model to 0, periodic model and growth model are trained with the historical data of the first 20 days, thus determining parameters.
- (4) Based on current load, periodic quantity model and load trend model, the loads to be forecasted are calculated, respectively.

5. Simulation and Predictable Time on the Mutual Influence of Three Chaotic Subsequences.

5.1. Influence of high-frequency chaos quantity on periodic quantity. The simulated quasi-periodic signal is used as follows:

$$x(t) = 5 \times (0.7 \times \sin(2\pi \times 50 \times t) + \sin(2\pi \times 100 \times t)) \quad (10)$$

Chaos quantity is simulated with logistic equation.

$$y(t) = 4 \times (1 - y(t - 1)) \times y(t - 1) \quad y(0) = 0.41 \quad (11)$$

Chaos quantity is

$$s(t) = x(t) + y(t) \quad (12)$$

Reconstruction of phase space: Delay time $\tau = 2$; dimension $m = 2$. Figs. 3 (1)-(3) show that after reconstruction.

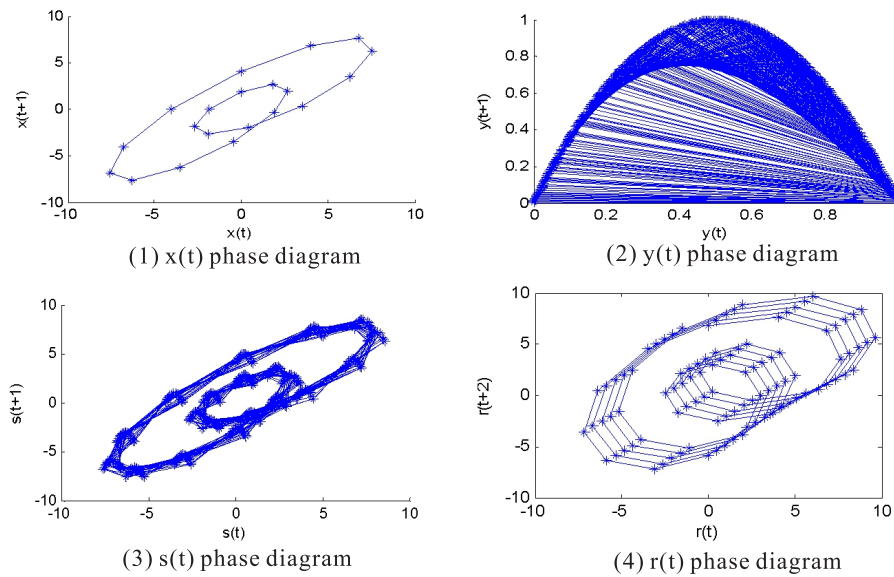


FIGURE 3. Phase diagram of each simulation quantity

TABLE 1. Number of adjacent points

| $x(t)$ | $y(t)$ | $r(t)=x(t)+z(t)$ | $s(t)=x(t)+y(t)$ |
|--------|--------|------------------|------------------|
| 394 | 336 | 245 | 394 |
| 254 | 308 | 366 | 254 |
| 334 | 341 | 265 | 214 |
| 374 | 369 | 394 | 334 |
| 234 | 313 | 386 | 374 |
| 274 | 346 | 225 | 274 |
| 314 | 244 | 346 | 406 |
| 354 | 360 | 353 | 314 |
| 214 | 260 | 333 | 234 |
| 294 | 403 | 285 | 354 |

Meanwhile, we calculate 10 Euclidean adjacent points of the 415th point in each phase space (See Table 1).

Fig. 3 and Table 1 illustrate it mainly show the characteristics of the leading periodic quantity in phase space. 80% adjacent points in $x(t)$ and $s(t)$ are the same, but there is no same point in $y(t)$ and $s(t)$. It does not reflect the characteristics of phase space of chaos quantity. Two components mutually affect the forecast accuracy.

5.2. Influence of seasonal variation quantity and development trend quantity to quasi-periodic quantity. Relatively, seasonal variation quantity and development trend quantity vary slowly, so direct current value (DC Value) is used for simulation.

$$z(t) = 25 \times t \quad (13)$$

$$r(t) = x(t) + z(t) \quad (14)$$

Fig. 2 (4) shows the 2-dimensional phase diagram ($\tau = 3$, and $m = 2$), and Table 1 shows 10 Euclidean adjacent points of the 415th point. There is only 1 same point for $r(t)$ and $s(t)$, and DC Value has obvious interference on periodic quantity.

5.3. Reason that load contains chaotic characteristics and simulation of predictable time. Load trend is simulated with sine function.

$$p(t) = 1000 \times \sin(2\pi \times 50 \times t) \quad (15)$$

Chaos quantity uses logistic equation for $y(t)$ simulation, let

$$z(t) = p(t) + y(t) \quad (16)$$

Obviously, $p(t)$ is the dominant quantity in $z(t)$. Laypunov indexes of $z(t)$ and $p(t)$ are $\lambda_z = 0.9732$ and $\lambda_p = 0.9993$, respectively, almost the same. Although the load trend is the dominant quantity, the obtained Laypunov index still fluctuates around load trend. It proves the rationality of reason analysis that the load has chaotic characteristics.

Multi-step prediction is used for $z(t)$, with the prediction of 96 steps (See Fig. 4). 0 is the actual value; * the predicted value.

Mean absolute error $E_{mape} = 0.1\%$.

Based on the reciprocal of Laypunov index, the predictive step of $z(t)$ is 1, inconsistent with the prediction.

It is not difficult to find that the predictive time of load, not only determined by chaos quantity, should consider the forecast time of load trend and chaos quantity. As to forecast method, we cannot simply determine chaos method is suitable for the time sequence containing chaos quantity. The other factors should be considered to select the

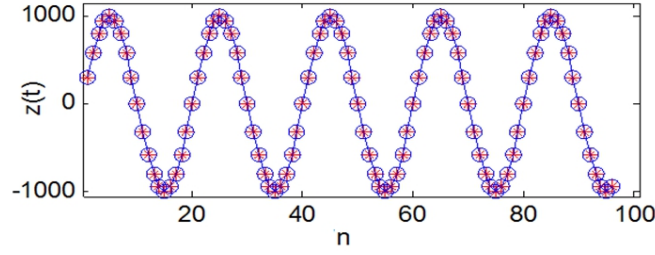


FIGURE 4. Actual curve and predicted curve of $z(t)$

appropriate method. In the prediction of $z(t)$, LS-SVM chaos prediction method is also suitable for the prediction of $p(t)$, thus deriving accurate prediction.

6. Case and Analysis of Load Forecasting.

6.1. **Single step forecasting of 1h.** The above method was used for the prediction and simulation of load data. The data recorded the loads of 365 days in the city; with the sampling period of 15min. Fig. 1 (1) shows the prediction of the load in the next 1h. The 110th to 120th days were used for training, and the 121st to 150th days for test, with the prediction of 720 points (regardless of weekdays and holidays). As a comparison, the original data without dividing into molecular model was forecasted with the mentioned periodic model, namely original model; the method with sampling period of 1h was called the method (2) in the work. Performance index of prediction is defined as follows.

$$E_{mse} = \sqrt{\frac{1}{n} \sum_{i=1}^n \left(\frac{L_i - L_i'}{L_i} \right)^2} \times 100\%; E_{mape} = \frac{1}{n} \sum_{i=1}^n \left| \frac{L_i - L_i'}{L_i} \right| \times 100\%; E_{ape} = \left| \frac{L_i - L_i'}{L_i} \right| \times 100\%$$

where E_{mape} is average relative error; E_{mse} the root mean square relative error; E_{ape} the absolute percent error; L_i and L_i' are the actual load and forecast load at a time, respectively.

TABLE 2. Parameters of models

| Error | Method in the work | Method in the work (2) | Original model |
|-----------------------|--------------------|------------------------|----------------|
| $E_{mse}(\%)$ | 1.21 | 1.30 | 1.93 |
| $E_{mape}(\%)$ | 0.88 | 0.96 | 1.40 |
| Maximum $E_{ape}(\%)$ | 4.99 | 5.60 | 11.74 |

TABLE 3. Error table

| Error | Periodic model | Load trend model |
|-----------------------|----------------|------------------|
| $E_{mse}(\%)$ | 2.78 | 142.97 |
| $E_{mape}(\%)$ | 2.19 | 78.13 |
| Maximum $E_{ape}(\%)$ | 7.48 | 693.68 |

Table 2 shows the parameters of forecasting model. τ and m are the delay time and embedding dimension calculated by mutual information method and Cao method; τ' and m' are the ones used in practice. Table 3 shows the comparison of forecast errors of two methods. For the point of $E_{ape} > 3\%$, the method in the work accounts for 0.35%, and the original model for 4.58%. Fig. 5 shows the error of each point.

The results show it improves the accuracy of original model and stability to divide the load into submodels for forecasting, compared with that of original model. The accuracy of the method in the work improves after increasing sampling frequency.

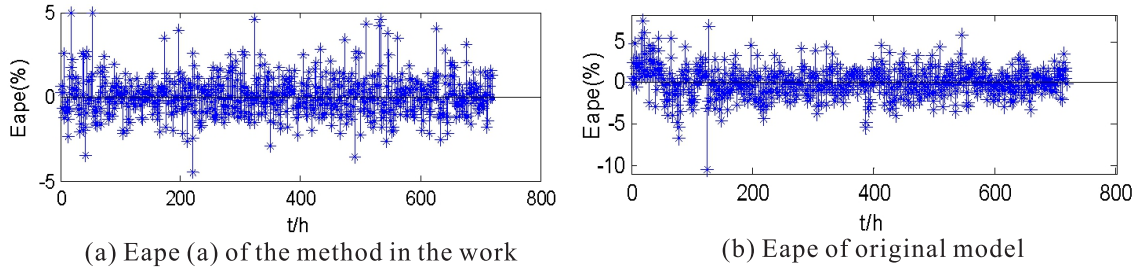


FIGURE 5. Forecast error

6.2. **Multi-step forecasting of 15min.** Periodic model was performed with multi-step forecasting of 15min for 121-123 days. Load trend model was forecasted for 121 days. Fig. 5 shows the errors; Fig. 6 the forecast and error cures; Fig. 6 the local errors of multi-step forecasting of trend model. The dotted line is the predicted value, and the solid line the actual value.

TABLE 4. Error table

| Parameter | Periodic model | Growth model | Original model |
|----------------|--------------------|--------------------|--------------------|
| τ / τ' | 15/4 | 21/4 | 12/4 |
| m / m' | 8/30 | 5/40 | 10/40 |
| γ | $3 * 10 \wedge 16$ | $3 * 10 \wedge 19$ | $3 * 10 \wedge 12$ |
| σ | 50 | 100 | 100 |

Table 4 shows periodic model can still maintain accuracy after multi-step forecasting for 3 days. Based on the reciprocal of Lyapunov index, predictive step is 14. Figs. 5 and 6 show the error of load trend model is below 10% in the first 16 steps. According to the reciprocal of Lyapunov index, predictive step is 18.

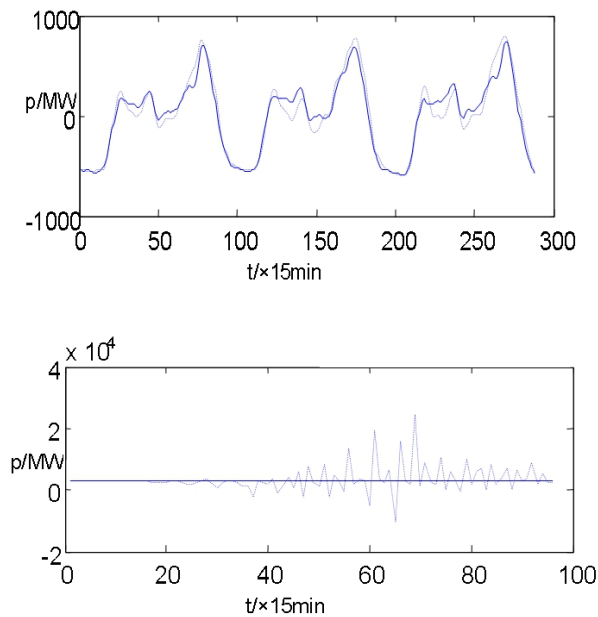


FIGURE 6. Actual curve and predicted curve of $z(t)$

The load trend of periodic model has strong periodicity, with weak influence from chaos quantity. Thus, predictable time is bigger than the value determined by the reciprocal of

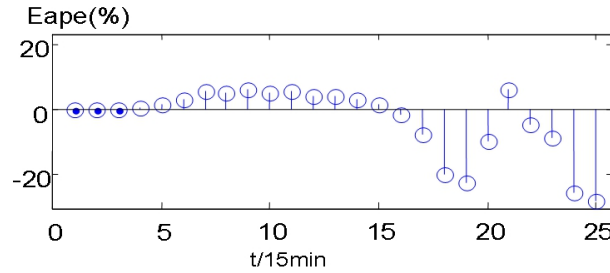


FIGURE 7. Actual curve and predicted curve of $z(t)$

Lyapunov index. Load trend model has poor regularity, with bigger influence from chaos quantity. Therefore, the actual predictable time approaches the value determined by the reciprocal of Lyapunov index. It proves the analysis in Section 2.5.

The results showed there was short time for multi-step forecasting with the method in the work due to poor regularity and short forecast time of load trend model. Forecast accuracy was significantly improved for short-time forecasting within 2h.

The method in the work used training data of 10 days to forecast the load of one month, proving the method has good stability of parameter and strong robustness.

7. Conclusions.

1. Based on the stationary wavelet decomposition, load sequence was decomposed into three sub-sequences, revealing the load contains the law of chaos.
2. LS-SVM was used to determine m and τ reconstructed by phase space of chaos quantity. It improved forecast accuracy to combine LS-SVM with local forecasting method of chaos. The actual load data was not pure chaos quantity, and the method was more practical.
3. The predictable steps of submodels and Lyapunov index showed the record data of load had chaos quantity and periodic quantity, and Lyapunov index could only be the predictable step of chaos quantity.

The actual data shows the method in the work, compared with undecomposed load data, has strong robustness, high robustness, good stability and practical value.

Acknowledgment. The work was supported by Key Projects of Science and Technology in Henan.

REFERENCES

- [1] [LIU Chenhui. Theories and methods of power system load forecasting. Harbin: Harbin Institute of Technology University Press, 2017.1-6.
- [2] Liang Zhishan, Wang Limin, Fu Dapeng et al. Electric power system short-term load forecasting using Lyapunov exponents technique. *Proceedings of the CESS*, 2018, 18(5): 368-371.
- [3] Li Tianyun, Liu Zifa. The chaotic property of power load and its forecasting. *Proceedings of the CSEE*, 2010, 20(11): 36-39.
- [4] Lu Jinhu, Zhan Yong, Lu Junan. The non-linear chaotic improved model of the electric power system short-term load forecasting. *Proceedings of the CSEE*, 2010, 20(12): 81-82.
- [5] [Jiang Chuanwen, Yuan Zhiqiang, Hou Zhijian et al. Research of forecasting method on chaotic load series with high embedded dimension. *Power System Technology*. 2014, 28(3): 25-28(in Chinese).
- [6] Yue Yihong, Han Wenxiu, Zhang Weibo. Local adding-weight linear regression forecasting method of chaotic series based on degree of incidence. *Proceedings of the CSEE*. 2014, 24(11):17-20.
- [7] WANG De-yi, YANG Zhuo, YANG Guo-qing. Short-term Load forecasting based on chaotic characteristic of loads and least squares support vector machines. *Power System Technology*. 2018, 32(7): 66-71.

- [8] LEI Shao-lan, SUN Cai-xin, ZHOU Quan, ZHANG Xiao-xing. The research of local linear model of short-term electrical load on multivariate time series. *Proceedings of the CSEE*. 2016, 26(2):25-29(in Chinese).
- [9] Yang Zhengling. Detection and prediction of chaos in time series and their applications in power systems [D]. Dissertation for Dr. Degree, Tianjin University, 2012.
- [10] Xiang Zheng, Zhang Tai-yi, Sun Jian-cheng. Prediction algorithm for laser chaotic based on stationary wavelet transform and reconstructed phase space. *Acta Photonica Sinica*, 2015, 34(11):1756-1759.
- [11] Ren R, Xu J, Zhu S H. Prediction of chaotic time sequence using least squares support vector domain. *Acta Phys Sin*, 2016, 55(2): 555-562.
- [12] Cui Wanzhao, Zhu Changchun, Bao Wenxing et al. Prediction of the chaotic time series using support vector machines. *Acta Physica Sinica*, 2014, 53(10):3303-3309.
- [13] Deng Naiyang, and Tian Yingjie. SVMs-the new method in data mining. *Science and Technology Press*, 2014, 71-94.
- [14] Suykens J A K, Vande walle J. Least squares supportvector machine classifiers. *Neural Processing Letters*. 2009, 9(3) 293-300.
- [15] Huang Yanwei, Wu Tihua, and Zhao Jingyi. System identification and simulation of SVM regression. *Computer Simulation*, 2014, 21 (5): 41-44.
- [16] H.Ksntz, T.Schreiber. Nonlinear time series analysis [M]. *Cambridge University Press*, 2016.
- [17] Liangyue Cao. Practical method for determining the minium embedding dimension of ascalar time series. *Physica D*, 2017, 110:43-50.
- [18] Lv Jinhua, Lu Jun'an and Chen Shihua. Analysis and application of chaos time series. *Wuhan: Wuhan University Press*, 2012: 85-92.
- [19] Yang Zhengling, Zhang Guangtao, Chen Hongxin et al. Parameter optimization in synthesizing load trend and chaotic components to short term load forecasting. *Power System Technology*, 2015, 29(4) 27-30.
- [20] Liu Han, Liu Ding, Ren Haipeng. Chaos control based on leastsquare support vector machines. *Acta Physica Sinica*, 2015, 54(9): 4019V4025.
- [21] Meng, Zhenyu, and Jeng-Shyang Pan. QUasi-Affine TRansformation Evolution with External ARchive (QUATRE-EAR): an enhanced structure for differential evolution. *Knowledge-Based Systems* 155 (2018): 35-53.
- [22] Meng, Zhenyu, and Jeng-Shyang Pan. Monkey king evolution: a new memetic evolutionary algorithm and its application in vehicle fuel consumption optimization. *Knowledge-Based Systems* 97 (2016): 144-157.